

Structural Analysis of MurG Interactions with Substrates, Inhibitors, and MraY

Thesis by
Helen Brackney

In Partial Fulfillment of the Requirements for
the degree of
Bachelor of Science in Chemical Engineering

The logo for the California Institute of Technology (Caltech), featuring the word "Caltech" in a bold, orange, sans-serif font.

CALIFORNIA INSTITUTE OF TECHNOLOGY
Pasadena, California

2024

©2023

Helen Brackney

ORCID: 0009-0009-8067-768X

ACKNOWLEDGEMENTS

I would like to thank my graduate student mentor Anna “Karen” Orta, for guiding and teaching me throughout my time as an undergraduate researcher. Karen has been a source of advice, freely giving encouragement and suggestions when they were needed.

I would also like to thank William Clemons Jr. for allowing me to join the lab that has been my research home and for giving me invaluable advice and suggestions on both research and my plans after graduating Caltech.

I also thank the Stanford Synchrotron Radiation Lightsource for the beamtime and x-ray crystal diffraction maps, the UCLA MBI- SERp Server for assistance in creating some of the protein mutants, and Beckman Imaging Facility for instrument support for the electron microscopy images and data.

For all my research time at Caltech, I’d like to thank all of the Clemons lab members for their support and advice throughout.

ABSTRACT

The peptidoglycan layer in bacterial cells is a popular target for antibiotic development. The membrane protein MraY and peripheral membrane protein MurG are part of critical steps in the synthesis of peptidoglycan. Lipid I, a lipid precursor formed by MraY, is recognized by MurG through its soluble domain. Currently, there is no structure of MurG with bound Lipid I, and the residues required for this interaction have not been conclusively defined. Crystallographic methods and Cryo-Electron Microscopy were applied to study the interactions between MurG and the soluble domain of Lipid I by binding Park's Nucleotide, Lipid II, or a Lipid I analog were used to study the interactions of MurG and MraY with the aforementioned substrates. By adding Park's Nucleotide, Murgocil, Lipid II, the Lipid I analog, or a combination of the listed additives to concentrated MurG, crystals formed under optimized conditions. We aim to obtain electron-density maps from these techniques to model the structure of MurG.

TABLE OF CONTENTS

Acknowledgements	iii
Abstract	iv
Table of Contents.....	v
List of Figures	vi
List of Tables.....	ix
Chapter 1: Introduction	1
Chapter 2: Mutation Design and Purification Optimization.....	3
2.1 MurG Mutations.....	3
2.2 Optimizing MurG Purification	3
2.3 Optimizing MraY Purification	4
Chapter 3: Discussion and Future Work	7
3.1 MurG Crystallization.....	7
3.2 MurG and MraY Interactions	13
Chapter 4: Methods.....	17
4.1 Protein Expression.....	17
4.2 Protein Purification via Affinity Column.	17
4.3 GFP Nanobody Pulldown.....	18
4.4 Crystal Trays Preparation.	19
4.5 UMP-Glo Assay	19
4.6 CryoEM Grid Preparation	20
4.7 Nanodisc Assembly and Purification	20
Bibliography	22
Appendix A: Constructs	24
A.1 His6- <i>Hy</i> MurG Protein Sequence.....	24
A.2 His6- <i>Hy</i> MurG SM2 Protein Sequence	24
A.3 His6- <i>Hy</i> MurG Mutant 17 Protein Sequence	25
A.4 His6- <i>Alg14TMD-Hy</i> MurG Protein Sequence	25
A.5 His6- <i>Ec</i> MurG Protein Sequence	26
A.6 His6- <i>Hy</i> MraY Protein Sequence.....	27
A.7 <i>Hy</i> MraY-GFP Protein Sequence	27
A.8 <i>Ec</i> MraY-His6 Protein Sequence	28

LIST OF FIGURES

<i>Number</i>		<i>Page</i>
1.1	The Peptidoglycan Biosynthesis Pathway. The family of Mur proteins synthesizes Park's Nucleotide. MraY adds an undecaprenyl phosphate to Park's Nucleotide. MurG attaches the UDP-GlcNAC and converts Lipid I to Lipid II before it gets flipped and pushed into the periplasm. (Adapted from Laddomada, F. <i>et al.</i>) ¹	2
2.1	HyMurG Mutants. Each mutation to the <i>HyMurG</i> sequence is shown in the color that is in the <i>HyMurG</i> structure. The TMD Mutation adds a trans-membrane domain to the protein that is pulled from the one of the subunits of mammalian analog of MurG: Alg14. Mutation 17 changes one of the hydrophobic residues (Tryptophan 76) in the region where MurG is bond to the membrane into an alanine releasing it from the membrane. The SM2 mutation mutates residues KNIK to AAAA.	4
2.2	MurG Nickel Column Purification Compared to Chitin Column Purification. The elutions from the nickel resin (A) came off with many contaminants and the elution after the chitin column (B) shows fewer contaminants. The elution on the right was filtered and further purified through size-exclusion chromatography.	5
2.3	MraY Nickel Column Purification Compared to GFP Pulldown Purification. The elutions from the nickel resin co-eluted with many contaminants (A) is shown compared to the elutions after the GFP pulldown purification (B). The GFP pulldown had a lower quantity of	5

contaminants though the relative abundance is higher. *HyMraY* was purified from the free anti-GFP nanobody *via* a size exclusion column.

- 3.1 **Three Stages of Data Collection. A. Crystal in a Well.** The first image shows the crystal in a well. The diameter of the image is 1.79 mm and the length of the scale in the middle of the image is 0.35 mm. **B. Crystal Frozen in a Loop.** After being fished out of the well shown in A, the crystal is frozen in liquid nitrogen. This image shows one of the crystals in A frozen in a 0.1 mm loop with some ice formed around the edges. **C. X-ray Diffraction Map.** After the crystal is diffracted with x-rays, scattered ray diffraction maps are collected and compiled to create electron density maps. From these maps, a structure of the protein crystallized can be produced. 9
- 3.2 **MurG Structure.** This 2.75 Å structure of MurG was created by processing x-ray diffraction maps. There are two copies of the protein shown, one is upright with the theoretical membrane binding site up and the other is rotated 180° along one axis and then 90° relative to the axis. 10
- 3.3 **Front View of single MurG Structure.** This is a front view of the 2.75 Å structure of MurG; the membrane binding site is oriented up and the binding pocket is on the left. 10
- 3.4 **Side View of single MurG Structure.** This is a side view of the 2.75 Å structure of MurG; the membrane binding site is oriented up and the binding pocket is in the front of the page. 11

- 3.5 **HyMraY and HyMurG TMD Nanodisc Purification.** **A.** The samples taken from intermittent steps of purification of the nanodisc via nickel column. The first half are samples from the elutions from the first removal of the solution from the Bio-beads and the second half is from a wash of the Bio-beads. **B.** Size exclusion chromatograph and corresponding SDS-page gel (C) samples are from the size exclusion column. The fractions in red were pooled and then frozen on copper grids for CryoEM. 15
- 3.6 **MraY and MurG Nanodisc Grid CryoEM Image.** There are few nanodisc particles shown in this frozen grid. The dark grey section in the upper right-hand corner is the copper grid background. The conditions for this grid were a Blot force of 4, a blot time of 7, and a concentration (measured at 1 Abs = 1 mg/mL) of 0.5 mg/mL. 16

LIST OF TABLES

Number		Page
3.1	HyMurG Crystal Data Statistics. The table of crystal data statistics shows the signal-to-noise ratio and the other factors of the data separated by resolution shell limit.	11
3.2	HyMurG Structure Statistics. These statistics of the <i>HyMurG</i> show its R-factors and its Ramachandran favored numbers. They also show the clash score and RMS of the bonds and the angles.	12
3.1	UMP-Glo Assay for <i>HyMraY</i> and <i>HyMurG</i>. Each row examines the activity of different protein-lipid combinations. With the expectation of the first and last rows, the first well shows the fluorescent of the protein by itself. The first row shows the fluorescence of decreasing dilutions of UMP. The first four wells in the last row have the same concentration of <i>HyMurG</i> protein with varying lipid buffers (none, Y55, Y20, and Y10 respectively). The last three wells have <i>HyMraY</i> and <i>HyMurG</i> dilutions with a substrate buffer and no lipids.	14

Chapter 1

Introduction

The need for more antibiotics grows more pressing with the number of antibiotic-resistant bacteria on the rise.² Consequently, there has been an increase in studies looking for antibiotic targets in bacteria. One such target is the bacterial peptidoglycan. The peptidoglycan is composed of polymers of sugars and amino acids that form a mesh-like layer outside of a bacterial wall to protect it. Without this layer successfully formed, the bacterial cell cannot properly divide which makes it an ideal target for antibiotics and inhibitors.³

The peptidoglycan synthesis process involves many different proteins, notably *MraY* and *MurG* (Fig. 1.1). It begins with UDP-N-acetylglucosamine (UDP-GlcNAc) in the cytoplasm of the cell and then a series of proteins (*MurA-F*) add multiple amino-acids converting it into uridine diphosphate-N-acetylmuramyl-pentapeptide (UDP-MurNAc-pentapeptide). *MraY* then catalyzes the donation of phosphor-MurNAc-pentapeptide to the lipid carrier undecaprenyl phosphate (C55-P) to form undecaprenyl pyrophosphoryl MurNAc-pentapeptide, or Lipid I. Lipid I is then transferred onto the peripheral membrane protein *MurG*. *MurG* is another essential protein for this synthesis process. It catalyzes the addition of GlcNAc onto Lipid I to form Lipid II, which is the essential subunit of the peptidoglycan layer.⁴ Lipid II is flipped into the periplasm by *MurJ* where it undergoes polymerization forming an alternating MurNAc and GlcNAc chain with cross-linking between the pentapeptides to form the peptidoglycan layer.

From functional analysis on *MraY*, the group has determined that the transfer from Lipid I to Lipid II happens quickly; there is an abundance of Lipid II relative to Lipid I in the native cell state.¹⁶ Based on this, *MraY* and *MurG* are likely colocalized in the membrane and may even form a complex.⁵ Looking at substrate transfer interactions between these two proteins would illuminate a key step in the Peptidoglycan Biosynthesis pathway.

The Clemons group has previously purified MurG and set up crystal trays with Park's Nucleotide and Murgocil (a lipid substrate mimic and inhibitor respectively), but no protein structures were obtained with either molecule on the MurG binding site. Based on the knowledge that MurG is responsible for the transformation of Lipid I to Lipid II, it is reasonable that there is an interaction between MurG and Lipid I or Lipid II.⁶ Crystallizing MurG with Lipid II would give insight into the interaction site of MurG that Lipid I targets. Using *Escherichia coli* MraY (*EcMraY*), *Escherichia coli* MurG (*EcMurG*), *Hydrogenivirga sp.* MraY (*HyMraY*), and *Hydrogenivirga sp.* MurG (*HyMurG*) the interaction can be characterized.

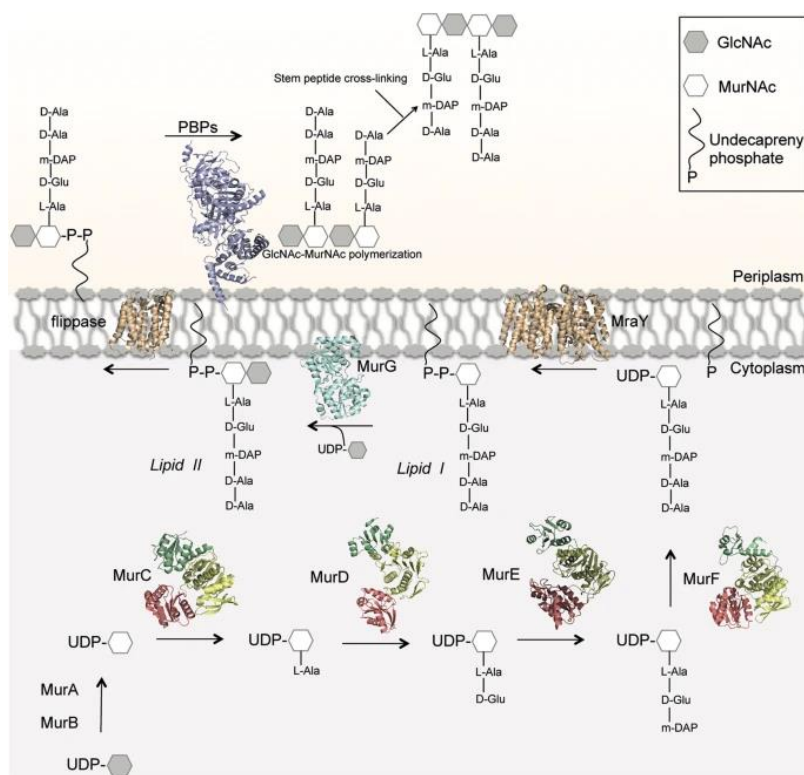


Figure 1.1. The Peptidoglycan Biosynthesis Pathway. The family of Mur proteins synthesizes Park's Nucleotide. MraY adds an undecaprenyl phosphate to Park's Nucleotide. MurG attaches the UDP-GlcNAc and converts Lipid I to Lipid II before it gets flipped and pushed into the periplasm. (Adapted from Laddomada, F. *et al.*)¹

Chapter 2

Mutation Design and Purification Optimization

2.1 MurG Mutations

To facilitate the purification and crystallization of HyMurG, several different mutants were used. A surface entropy reduction software created at UCLA was used to determine the best locations for mutations to create a protein with reduced surface entropy.⁷ These surface entropy mutants are designed to crystallize better because they reduce the entropy between crystallographic subunits. Surface Mutant 2 (SM2) is a surface entropy mutant, shown in light purple in Figure 2.1. Similarly, we designed mutants that would allow for the purification of MurG from the cytoplasmic fraction, rather than the membrane. Mutant 17 is a point mutation that releases MurG from the cell membrane. This mutation makes it possible to purify *HyMurG* from the soluble rather than the membrane fraction and increase protein yield.

To assay the interactions between MurG and MraY within the membrane, a transmembrane domain was added to the N-terminus of MurG. As a peripheral membrane protein, MurG may associate and dissociate from the membrane through unknown mechanisms. By embedding MurG in the membrane, we aim to elucidate the interaction between MraY and MurG can be witnessed by creating a nanodisc with both proteins and, via CryoEM, analyzing the structure.

2.2 Optimizing MurG Purification

The three membrane-localized MurG strains (the wildtype, SM2 mutant, and MurG with the TMD) purified with a cobalt or nickel column and followed by size exclusion chromatography (see section 4.2). The soluble mutant (MurG 17) had contaminants present after the nickel column, therefore a chitin column was used. The chitin column bound most of the contaminants in the MurG 17 elution and after filtering, it was further purified through on the size exclusion chromatography.

2.3 Optimizing MraY Purification

Different tags in MraY were tested in attempts to purify the protein. The six-histidine-tag (His-tag) and Green Fluorescent Protein tag (GFP tag) had different affinities that led to various levels of purity. The nickel column with its histidine affinity pulled several contaminants, shown in Figure 2.3. The GFP pulldown purification, which uses a nanobody with affinity to GFP followed by a Small Ubiquitin-like Modifier (SUMO) cleavage resulted in a cleaner elution.

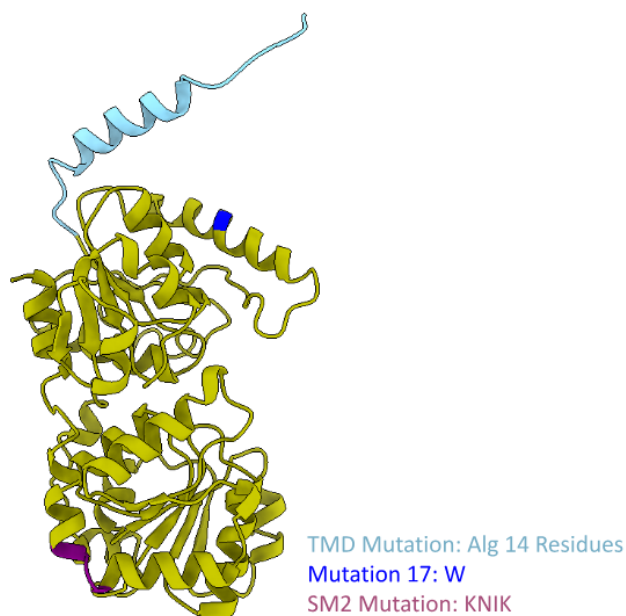


Figure 2.1. HyMurG Mutants. Each mutation to the *HyMurG* sequence is shown in the color highlighted in the *HyMurG* structure. The TMD Mutation adds a trans-membrane domain to the protein that is pulled from the one of the subunits of mammalian analog of MurG: Alg14. Mutation 17 changes one of the hydrophobic residues (Tryptophan 76) in the region where MurG is bond to the membrane into an alanine releasing it from the membrane. The SM2 mutation mutates residues KNIK to AAAA.

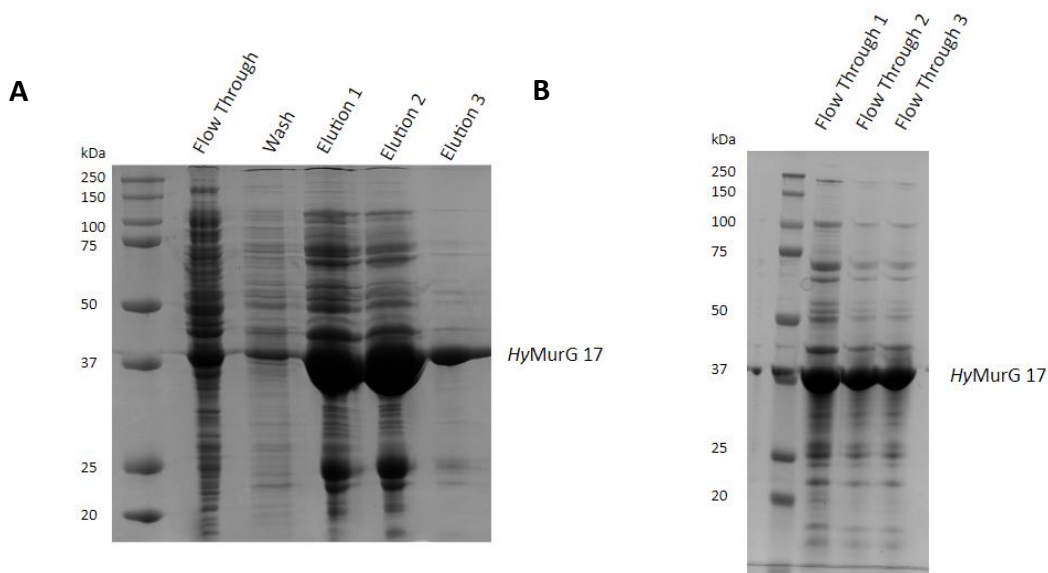


Figure 2.2. MurG Nickel Column Purification Compared to Chitin Column Purification. The elutions from the nickel resin (A) came off with many contaminants and the elution after the chitin column (B) shows fewer contaminants. The elution on the right was filtered and further purified through size-exclusion chromatography.

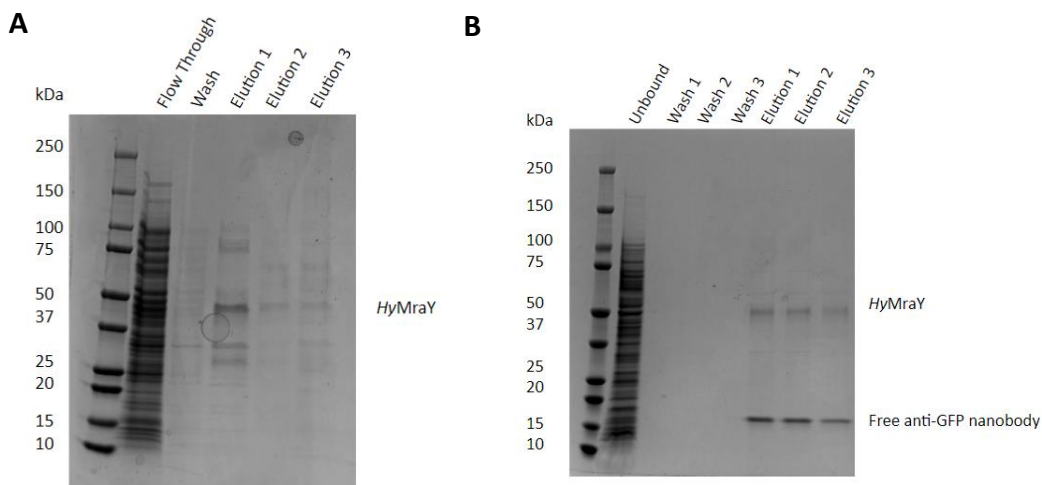


Figure 2.3. MraY Nickel Column Purification Compared to GFP Pulldown Purification. The elutions from the nickel resin co-eluted with many contaminants (A) is shown compared to

the elutions after the GFP pulldown purification (B). The GFP pulldown had a lower quantity of contaminants though the relative abundance is higher. *HyMraY* was purified from the free anti-GFP nanobody *via* a size exclusion column.

Chapter 3

Discussion and Future work

3.1 MurG Crystallization

Different crystallography methodologies were used, and each worked towards the optimization of the crystals. The type of the crystals obtained was dependent on the drop type, concentration of protein, concentration of substrate, concentration of additive, conditions in the mother liquor (precipitant, salt and buffer), microseeding, and macroseeding. Many distinct types of crystals were observed: needles, plates, and three-dimensional. Additive screens were also used on specific conditions from the JCSG+ Crystal screen (0.2 M potassium formate with 20 % w/v PEG 3350 and 0.2 M ammonium nitrate with 20 % w/v PEG 3350) to further optimize the crystal well conditions to form three-dimensional crystals which could contribute to future directions.

After purifying and crystallizing MurG in a variety of conditions, several crystals were fished and shipped to the Stanford Synchrotron Research Laboratory. X-rays are shot at the crystal and the crystal diffraction pattern is detected on a plate. The crystal is rotated 360° and the collection of maps is converted to electron density maps *via* Fourier Transforms. The statistics of the initial data set are shown in Table 3.1. Using Molecular replacement (and Matthew's Coefficient of 2) in Phenix, a structure of HyMurG is fitted into the electron density maps and then refined with Phenix and Coot.^{8,9} The refinement process was finished when the R-free factor began to rise with each round of refinement.

The final structure was resolved to a 2.75 Å resolution (Figure 3.2). The statistics of the structure improved with each refinement (Table 3.2). The condition in which the crystal formed was 5 mg/mL HyMurG SM2, 0.3 M Magnesium chloride hexahydrate; 0.3 M Calcium chloride dihydrate, 0.2 M Sodium HEPES pH 7.5, 0.2 M MOPS (acid) pH 7.5, 37.5 % v/v Precipitant Mix 4 (25% v/v MPD; 25% PEG 1000; 25% w/v PEG 3350) using the Morpheus Screen by Molecular Dimensions.¹⁰

For the future work for this project is obtaining a structure with a higher resolution and a clearly identifiable bonded Murgocil, Lipid I, Lipid II, or Park's Nucleotide. The next step is optimizing crystal tray conditions for crystallizing the substrates. Using other crystal screening conditions or additional additive screens to further optimize the crystallization are also options to pursue. Trays with different cryoprotectants and combinations of substrate mimics and inhibitors (like using UDP-GlcNAC in addition to Park's Nucleotide or Murgocil) or potentially other mutants of *HyMurG* might yield different amounts of protein during expression or facilitate the structure analysis of *HyMurG* through Cryo-EM or crystallographic methods.

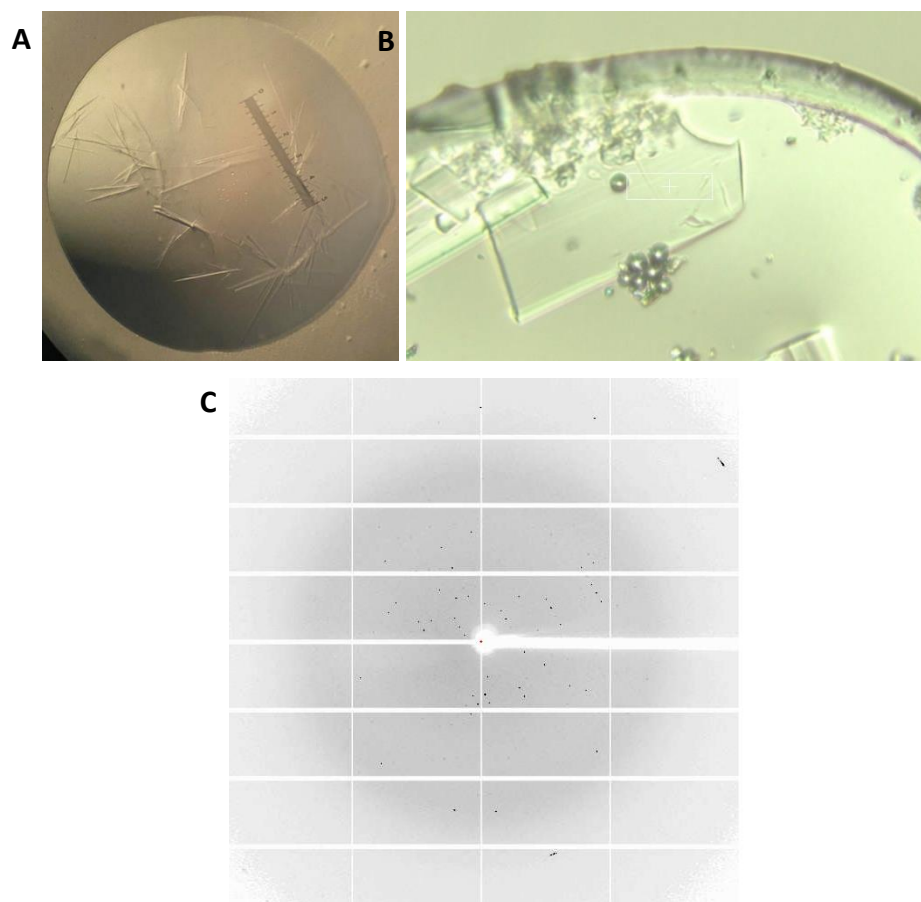


Figure 3.1. Three Stages of Data Collection. A. Crystal in a Well. The first image shows the crystal in a well. The diameter of the image is 1.79 mm and the length of the scale in the middle of the image is 0.35 mm. **B. Crystal Frozen in a Loop.** After being fished out of the well shown in A, the crystal is frozen in liquid nitrogen. This image shows one of the crystals in A frozen in a 0.1 mm loop with some ice formed around the edges. **C. X-ray Diffraction Map.** After the crystal is diffracted with x-rays, scattered ray diffraction maps are collected and compiled to create electron density maps. From these maps, a structure of the protein crystallized can be produced.

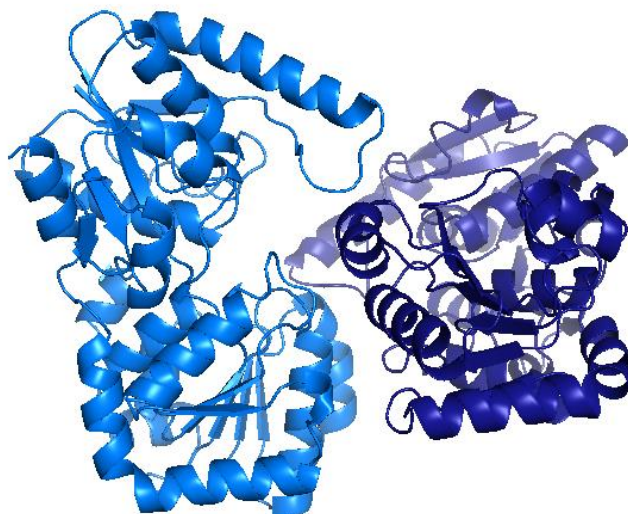


Figure 3.2. MurG Structure. This 2.75 Å structure of MurG was created by processing x-ray diffraction maps. There are two copies of the protein shown, one is upright with the theoretical membrane binding site up and the other is rotated 180° along one axis and then 90° relative to the axis.

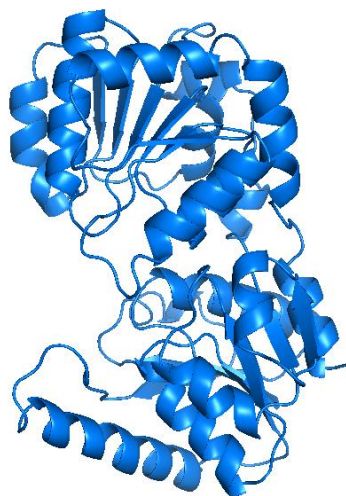


Figure 3.3. Front View of single MurG Structure. This is a front view of the 2.75 Å structure of MurG; the membrane binding site is oriented up and the binding pocket is on the left.

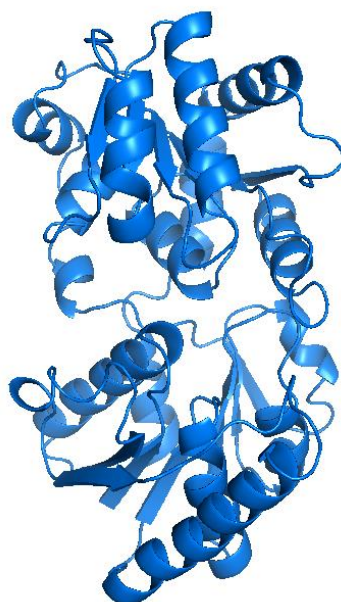


Figure 3.4. Side View of single MurG Structure. This is a side view of the 2.75 Å structure of MurG; the membrane binding site is oriented up and the binding pocket is in the front of the page.

Shell limit	Lower Angstrom	Upper	Average I	Average error	stat.	Chi**2	R-fac	R-fac	Linear	Square	Rmeas	Rpim	CC1/2	CC*
29.00	7.42		2243.8	44.1	31.5	4.148	0.066	0.073	0.073	0.073	0.029	0.996	0.999	
7.42	5.91		722.5	25.7	23.2	2.156	0.102	0.109	0.111	0.111	0.043	0.991	0.998	
5.91	5.17		737.1	29.8	27.4	1.912	0.118	0.123	0.128	0.128	0.048	0.987	0.997	
5.17	4.70		1031.0	38.4	34.9	2.153	0.114	0.119	0.124	0.124	0.047	0.989	0.997	
4.70	4.36		1060.3	43.1	39.5	2.209	0.127	0.135	0.138	0.138	0.052	0.987	0.997	
4.36	4.11		969.3	50.2	46.8	1.804	0.135	0.135	0.148	0.148	0.059	0.988	0.997	
4.11	3.90		752.1	52.3	49.9	1.547	0.164	0.156	0.180	0.180	0.071	0.983	0.996	
3.90	3.73		565.7	51.4	49.9	1.386	0.221	0.755	0.240	0.240	0.093	0.980	0.995	
3.73	3.59		514.0	54.4	53.2	1.163	0.234	0.256	0.255	0.255	0.099	0.971	0.992	
3.59	3.46		426.5	56.1	55.2	0.968	0.274	0.263	0.298	0.298	0.114	0.968	0.992	
3.46	3.36		363.3	59.0	58.3	1.092	0.323	0.691	0.352	0.352	0.139	0.939	0.984	
3.36	3.26		272.2	58.2	57.7	0.678	0.373	0.355	0.406	0.406	0.159	0.947	0.986	
3.26	3.17		220.6	60.4	60.1	0.683	0.429	0.453	0.469	0.469	0.187	0.931	0.982	
3.17	3.10		181.4	61.3	61.1	0.556	0.487	0.474	0.534	0.534	0.213	0.893	0.971	
3.10	3.03		159.2	61.9	61.7	0.555	0.536	0.511	0.589	0.589	0.237	0.878	0.967	
3.03	2.96		134.0	63.1	63.0	0.516	0.568	0.550	0.624	0.624	0.253	0.865	0.963	
2.96	2.90		114.3	62.5	62.4	0.516	0.676	0.705	0.746	0.746	0.310	0.756	0.928	
2.90	2.85		105.7	67.5	67.4	0.517	0.691	0.691	0.770	0.770	0.333	0.757	0.928	
2.85	2.80		101.5	66.5	66.4	0.501	0.701	0.651	0.789	0.789	0.353	0.769	0.932	
2.80	2.75		89.4	67.8	67.7	0.495	0.818	0.777	0.924	0.924	0.418	0.700	0.907	
All reflections			552.7	53.3	51.4	1.390	0.184	0.213	0.201	0.201	0.080	0.971	0.993	

Table 3.1. HyMurG Crystal Data Statistics. The table of crystal data statistics shows the signal-to-noise ratio and the other factors of the data separated by resolution shell limit.

Resolution (Å)	27.99 - 2.75
R-work	0.1897
R-free	0.2743
RMS (bonds)	0.014
RMS (angles)	1.452
Clashscore	10.35
Ramachandran favored (%)	94.36
Ramachandran outliers (%)	0.58
Rotamer outliers (%)	2.30

Table 3.2. HyMurG Structure Statistics. These statistics of the HyMurG show its R-factors and its Ramachandran favored numbers. They also show the clash score and RMS of the bonds and the angles.

3.2 MurG and MraY Interactions

The UMP-Glo assay is designed to show the activity of proteins whose function produces free UMP. The UMP-Glo enzyme fluoresces based on the amount of free UMP in the solution, produced by the breakdown of Park's Nucleotide or UDP-GlcNAc. An assay with *Escherichia coli* MraY (*EcMraY*) and *Escherichia coli* MurG (*EcMurG*) showed that the *EcMraY* was inactive. To rule out the possibility of this due to freezing, the assay was repeated with *HyMraY* and *HyMurG*; there was a change in species due to plasmid limitations. Based on the results shown in Table 3.1, *HyMraY* was also inactive despite being fresh from the concentrator tube. The wells with *HyMraY* and *HyMurG* had the most activity.

The two proteins were evaluated with three different lipids in solution. Each solution shown in Table 3.1 has a letter and number combination. If there is a "G", the solution has a 125 μ M concentration of UDP-GlcNAc. The letter "Y" indicates that there is a 125 μ M concentration of Park's Nucleotide and a 125 μ M concentration of a lipid. The number is the number of carbons in the lipid backbone (C55, C20, or C10). In the case of the wells H5, H6, and H7, the solution is only 125 μ M of Park's Nucleotide and 125 μ M of UDP-GlcNAc; there intentionally was no lipid as a control to measure the background free-UMP.

To capture the activity between MurG and MraY, nanodiscs were assembled. After the assembling a nanodisc ¹¹, the complex was purified via nickel affinity column and size exclusion chromatography (Fig.3.3). Post purification, the nanodiscs were frozen on Quantifoil Copper 1.2/1.3 grids for CryoEM analysis. The ice conditions were not optimal on the grids, and it was difficult to see particles or any nanodiscs that were correctly assembled (Figure 3.4). Because there were few particles from on the grid, the freezing

conditions (blot time, freezing time, and concentration of nanodisc) must be optimized for future work in classifying any interaction between MurG and MraY.

		1	2	3	4	5	6	7
UMP Control	A	51055.41	21286.37	16205.47	11050.03	4209.24	5548.826	7536.465
<i>HyMraY</i> with Y55	B	109.734	349.907	105.593	130.439	62.114	47.621	20.705
<i>HyMraY</i> with Y20	C	45.55	84.889	91.1	68.325	37.268	37.268	8.282
<i>HyMraY</i> with Y10	D	14.493	22.775	99.382	49.691	26.916	14.493	10.352
<i>HyMraY</i> and <i>HyMurG</i> with YG55	E	101.452	902.719	552.812	1101.483	602.503	354.048	95.241
<i>HyMraY</i> and <i>HyMurG</i> with YG20	F	66.255	1331.304	490.698	428.585	202.905	258.807	345.766
<i>HyMraY</i> and <i>HyMurG</i> with YG10	G	53.832	1053.863	815.76	1171.879	519.685	287.794	140.791
<i>HyMurG</i>	H	113.875	84.889	60.043	72.466	513.473	616.996	645.983

Table 3.3. UMP-Glo Assay for *HyMraY* and *HyMurG*. Each row examines the activity of different protein-lipid combinations. With the expectation of the first and last rows, the first well shows the fluorescence of the protein by itself. The first row shows the fluorescence of decreasing dilutions of UMP. The first four wells in the last row have the same concentration of *HyMurG* protein with varying lipid buffers (none, Y55, Y20, and Y10 respectively). The last three wells have *HyMraY* and *HyMurG* dilutions with a substrate buffer and no lipids.

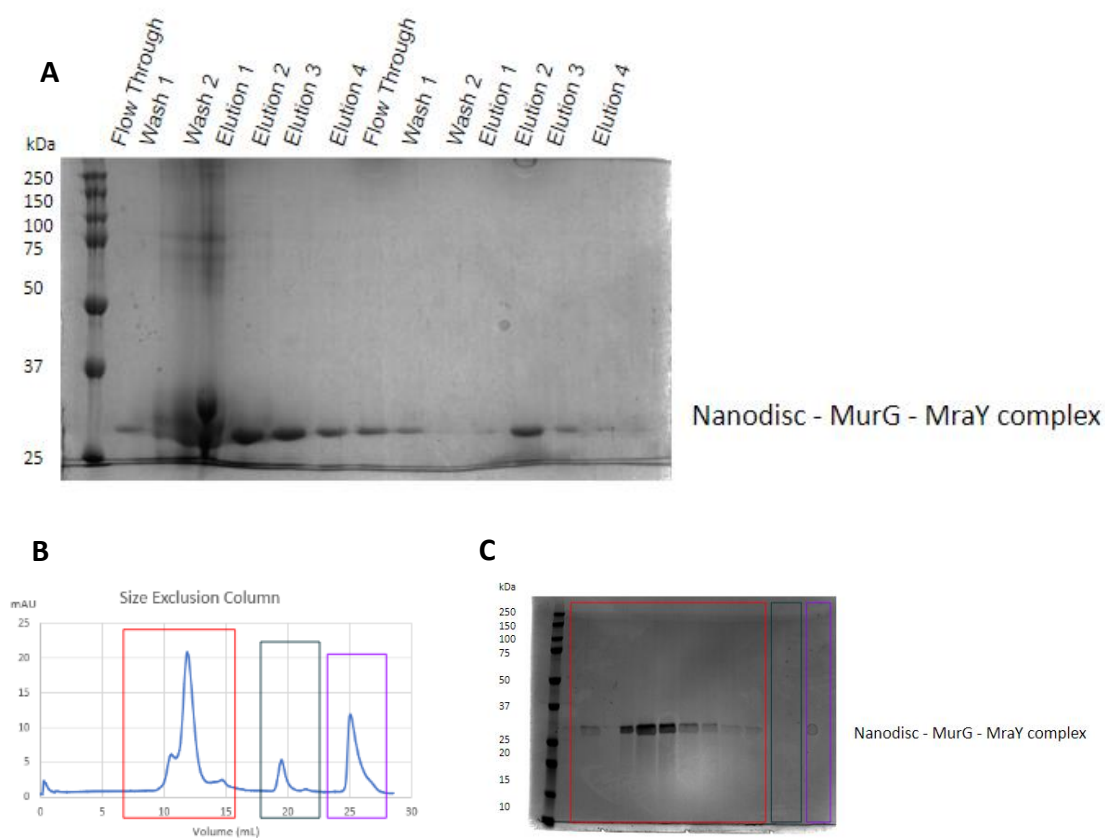


Figure 3.5. *HyMurA* and *HyMurG* TMD Nanodisc Purification. **A.** The samples taken from intermittent steps of purification of the nanodisc via nickel column. The first half are samples from the elutions from the first removal of the solution from the Bio-beads and the second half is from a wash of the Bio-beads. **B.** Size exclusion chromatograph and corresponding SDS-page gel (C) samples are from the size exclusion column. The fractions in red were pooled and then frozen on copper grids for CryoEM.



Figure 3.6. MraY and MurG Nanodisc Grid CryoEM Image. There are few nanodisc particles shown in this frozen grid. The dark grey section in the upper right-hand corner is the copper grid background. The conditions for this grid were a Blot force of 4, a blot time of 7, and a concentration (measured at 1 Abs = 1 mg/mL) of 0.5 mg/mL.

Chapter 4

Methods

4.1 Protein Expression.

A plasmid containing the gene to express the chosen protein (a MurG mutant or MraY mutant) is incubated with the competent cells (NiCO, NiMO, or LEMO) on ice and then heat shocked for thirty seconds before being incubated on the ice for five minutes. These primary contaminants for His-tagged proteins in these cells lines also have chitin-binding domains for later purification. The cells are then allowed to recover in LB (Luria Broth) at 37°C with shaking at 225 RPM. After an hour, the cells are plated on an LB agar plate with the antibiotic selection and allowed to grow overnight. The cells are resuspended in 30 milliliters of Luria-Bertani media and 5 mL of the mixture is aliquoted into a liter of 2xTY media (an autoclaved solution of one liter of water, 16 grams of tryptone, 10 grams of yeast extract, and 5 grams of sodium chloride). Then the cells are incubated at 37°C and 225 RPM with optical density (OD) checks at a 600 wavelength every hour.

When the OD reaches 0.70, the cells are ready to stop growing and start expressing the recombinant gene. For gene expression, each liter of media and cells is induced with 400 μ L of 1 M isopropylthio- β -galactoside (IPTG) (final concentration of 0.4 mM) followed by incubation at 30°C for four hours at 225 RPM. To separate the cells from the media, the cultures are centrifuged at 6000 RPM for ten minutes. The cell pellet is collected and then flash-frozen in liquid nitrogen.

4.2 Protein Purification via Affinity Column.

The cell pellet is thawed on ice and then resuspended with 10 mL of lysis buffer (20 mM tris pH 7.5, 300 mM NaCl, 10% glycerol, 5 mM beta-mercaptoethanol (BME), 1x phenylmethanesulfonyl fluoride (PMSF), and 1x benzamidine) per 1 g of cells. After being microfluidized, the cells are spun at 12000 RPM for twenty minutes to clear the lysate of

insoluble debris. After removing the debris pellet, the lysate is spun again at 38000 RPM for 30 minutes in an ultracentrifuge. This separates the solution into soluble proteins (proteins in the cytoplasm of the cell) and proteins in the membrane of the cell. When the protein was expected in the soluble fraction, it was mixed directly with cobalt or nickel resin beads. If the protein was expected in the membrane fraction, it was first solubilized with extraction buffer (20 mM Tris pH 7.5, 300 mM NaCl, 10% glycerol, 10 mM imidazole, 1% DM, 5 mM BME, 1x PMSF, and 1x benzamidine). Followed by a 1 hour incubation with the resin. The wash buffer (20 mM HEPES pH 7.5, 300 mM NaCl, 5% glycerol, 30 mM imidazole, 0.15% DM, 5 mM BME, 1x PMSF, and 1x benzamidine) was then flowed through to remove any weakly bonded proteins or any contaminants that did not go through the filter the first time. The elution buffer (20 mM HEPES pH 7.5, 150 mM NaCl, 5% glycerol, 200 mM imidazole, 0.15% DM, 5 mM BME, 1x PMSF, and 1x benzamidine) is then flowed through in three increments (5mL, 5mL, and 10mL) containing the purified protein. The His-tagged protein is eluted and can then be analyzed through an SDS-gel for purity. In each case of purification, the three elutions were concentrated before size exclusion chromatography. The column results can be analyzed through another SDS-gel to determine which fractions have protein that can be concentrated to use for crystal trays or for CryoEM grids.

4.3 GFP Nanobody Pulldown

The Green Fluorescent Protein (GFP) tag added to the C-terminus of HyMraY binds to a nanobody that binds to magnetic Streptavidin beads. 363 μ L of the beads are added to a 1.5 mL Eppendorf and the beads are washed with water. To remove any excess liquid, the tube is placed on a magnetic rack so that the liquid can be pipetted out, leaving the beads behind. The beads are then equilibrated in the solubilization buffer (20 mM HEPES pH 7.5, 150 mM NaCl, 5% glycerol, 0.15% DM, 5 mM BME, 1x PMSF, and 1x benzamidine). 20 μ L of the anti-GFP nanobody was incubated with the beads for 1 hour before the free anti-GFP

nanobody was removed. 1 mL of 50 μ M biotin in the solubilization buffer is incubated with the beads for five minutes and then the beads are washed with 1 mL of solubilization buffer.

The beads are resuspended in 500 μ L of solubilization buffer before being transferred to a 50 mL falcon tube that has solubilization protein in it and incubated for 1.5 hours. The beads are collected at the bottom of the falcon tube and the excess buffer is removed (50 μ L kept). The beads are resuspended in 1 mL of solubilization buffer and transferred to a 1.5 mL Eppendorf. They are then washed three times with solubilization buffer before being incubated in a solubilization buffer containing 0.5 μ M SUMO Eu1 protease for thirty minutes. The elutions are then collected and transferred to a 1.5 mL tube. The tube is spun at 21000xg minimum for ten minutes to pellet any remaining beads and the supernatant is run on a size exclusion column.

4.4 Crystal Trays Preparation.

Two types of crystal trays were set up (96 and 24 wells) with various conditions (JCSG+ Crystal Screen¹², Morpheus Crystal Screen¹⁰, Crystal Hit Screen¹³, and Index Crystal Screen¹⁴). Multiple techniques were used (micro-seeding, hanging drop, sitting drop) to create crystals that are were large and clear enough to fish. The micro-seeding technique involved micro-pipetting a crystal tray well with crystals into an Eppendorf tube with a seed bead and then vortexing at high speed for 90 seconds. The seeds are then picked up by dipping a cat's whisker in the solution and then drawing the whisker through the hanging drop. The hanging drop is suspended from the well cover whilst the sitting drop sits in a carrier under the well cover.

4.5 UMP-Glo Assay

The assay was prepared by setting up a 96 well plate with the chosen substrates and proteins in solution. The final concentration of protein in the first well was 10 μ M and each

sequential well had one half of the concentration in the previous well (via sequential dilution before the substrates are added). The solutions were allowed to equilibrate for thirty minutes and then 25 μL of UMP-Glo enzyme was added to each well. The assay plate was placed on a plate shaker to mix for 60 seconds. It was then incubated at room temperature for one hour before obtaining luminescence readings with a plate reader.

4.6 CryoEM Grid Preparation

30 μL of the specified protein concentration is prepared. After the equipment is cooled with liquid nitrogen, a 3 μL sample is pipetted onto the grid and was blotted with specific blot time and force (determined by protein concentration and ice buildup) before being plunged into liquid ethane followed by liquid nitrogen. The first round of grid freezing was with a blot time of 3.5 seconds and a blot force of 8 and the second round was with a blot time of 4 second and a blot force of 7.

4.7 Nanodisc Assembly and Purification

After calculating the membrane protein of interest (MPI): membrane scaffolding protein (MSP): lipid ratio,¹⁷ 10 μM of MurG, 10 μM of MraY, and 40 μM of MSP1E3D1 is incubated with 3 mM of 1,2-dimyristoyl-sn-glycero-3-phosphocholine (DMPC) and 100 μL of 20 mM MSP cholate (sodium cholate dissolved in MSP buffer (20 mM Tris pH 7.5, 100 mM NaCl, and 0.5 mM EDTA) and then diluted to a final volume of 500 μL with MSP buffer. This protein solution was allowed to rock at 4°C for one hour. After transferring 250 mg of Bio-Rad Bio-Beads SM-2 Absorbents into an Eppendorf tube, the beads are washed twice in water by added 600 μL to the Eppendorf, vortexing on high for ten seconds, centrifugation for ten seconds using a tabletop centrifuge, and then pipetting out as much liquid as possible without removing beads. This process is repeated twice with 600 μL of MSP buffer.

The protein solution is added to the beads and incubated for at least four hours on a rocker at 4°C. The solution is centrifuged a tabletop centrifuge and the solution removed and incubated with nickel resin for one hour at 4°C. The beads are washed with 600 μL of MSP

buffer and this wash is also incubated with nickel beads. The elution buffer is 2 mL of MSP buffer and supplemented with 2 mL of 1 M Imidazole; the nanodisc-protein complex is eluted in four aliquots of 500 μ L. The aliquots are concentrated and then loaded onto a size exclusion column to remove any final unbound protein or empty nanodiscs.

Bibliography

1. Laddomada, F. *et al.* The MurG glycosyltransferase provides an oligomeric scaffold for the cytoplasmic steps of peptidoglycan biosynthesis in the human pathogen *Bordetella pertussis*. *Sci. Rep.* **9**, 4656 (2019).
2. WHO publishes list of bacteria for which new antibiotics are urgently needed. <https://www.who.int/news/item/27-02-2017-who-publishes-list-of-bacteria-for-which-new-antibiotics-are-urgently-needed>.
3. Vollmer, W., Blanot, D. & de Pedro, M. A. Peptidoglycan structure and architecture. *FEMS Microbiol. Rev.* **32**, 149–167 (2008).
4. Mitachi, K. *et al.* Substrate Tolerance of Bacterial Glycosyltransferase MurG: Novel Fluorescence-Based Assays. *ACS Infect. Dis.* **6**, 1501–1516 (2020).
5. Mohammadi, T. *et al.* The essential peptidoglycan glycosyltransferase MurG forms a complex with proteins involved in lateral envelope growth as well as with proteins involved in cell division in *Escherichia coli*. *Mol. Microbiol.* **65**, 1106–1121 (2007).
6. Oluwole, A. O. *et al.* Peptidoglycan biosynthesis is driven by lipid transfer along enzyme-substrate affinity gradients. *Nat. Commun.* **13**, 2278 (2022).
7. Toward rational protein crystallization: A Web server for the design of crystallizable protein variants - PubMed. <https://pubmed.ncbi.nlm.nih.gov/17656576/>.
8. Adams, P. D. *et al.* PHENIX: a comprehensive Python-based system for macromolecular structure solution. *Acta Crystallogr. D Biol. Crystallogr.* **66**, 213–221 (2010).

9. Emsley, P. & Cowtan, K. Coot: model-building tools for molecular graphics. *Acta Crystallogr. D Biol. Crystallogr.* **60**, 2126–2132 (2004).
10. Morpheus I. *Molecular Dimensions* <https://moleculardimensions.com/en/category/16>.
11. Li, M. J., Atkins, W. M. & McClary, W. D. Preparation of Lipid Nanodiscs with Lipid Mixtures. *Curr. Protoc. Protein Sci.* **98**, e100 (2019).
12. JCSG Plus. *Hampton Research* <https://hamptonresearch.com/product-JCSG-Plus-901.html>.
13. Crystal Screen HT. *Hampton Research* <https://hamptonresearch.com/product-Crystal-Screen-Crystal-Screen-2-Crystal-Screen-HT-1.html>.
14. Index HT. <https://hamptonresearch.com/product-Index-Index-HT-5.html>.
15. Gao, X.-D., Tachikawa, H., Sato, T., Jigami, Y. & Dean, N. Alg14 Recruits Alg13 to the Cytoplasmic Face of the Endoplasmic Reticulum to Form a Novel Bipartite UDP-N-acetylglucosamine Transferase Required for the Second Step of N-Linked Glycosylation*. *J. Biol. Chem.* **280**, 36254–36262 (2005).
16. van Heijenoort, J. Lipid Intermediates in the Biosynthesis of Bacterial Peptidoglycan. *Microbiol. Mol. Biol. Rev. MMBR* **71**, 620–635 (2007).
17. Efremov, R. G., Gatsogiannis, C. & Raunser, S. Lipid Nanodiscs as a Tool for High-Resolution Structure Determination of Membrane Proteins by Single-Particle Cryo-EM. *Methods Enzymol.* **594**, 1–30 (2017).

Appendix A: Constructs

A.1 His6-*Hy*MurG Protein Sequence

ATGCACCACCACCACCACCACGGTCTGGTCCGCGTGGTCTAGGCTTCTCGTATCAGGAGGAGGAACAGG
AGGACACTTCTTCCCAGCTCTTGAGGTTCTCGCGAGAGCCGCGGCGGGCAGGCGGGCATACTACCCTCTACGTAG
GCGCCCAGAGAGGCATAGAGAGGGGCTTTGAGCACGCCATACCCGGTGCGGCGCTCTTCTTGAGCTTTA
CCCCTTCAGGGGGGTATCCGTTGGAGCACGGGTGGCGGCCCTACTGAGCTTCTGGAGAGGTATTTCCATT
TGAGGAGCCATACGCAGGGGGATTTAGGACGCTCGTATTCGGAGGTTATCCGAGTGTTCCAGCCGGTGT
TCACACGGTCCTCAAGAGAAAGCCCCTTACCTGCACGAACAGAACTCAGTGCCGAGCATGACCAACAGAC
TCCTCTCCCATTTCCGAGGAAGGTCTTTATAACCTTTGAGCACTCACGGAAGTCTTCAGGGGCATGAAG
GTGGTAAGGACAGGACTGCCGATAAGGGAAGAGCTCATAAACACCGCGCTTGACAAGTCCAACGCCAAG
GAAGCGCTCGGCTTCAAACCTGAGGCACCCCTGGTGCTTTCATGGGCGGCAGTCAGGGGGCAAGATTTA
TAAACAACCTCGCGGTAGACTTCGCCAAGAAGACCGGCGCACCGGTTCTGCTCTTGCTGGAGAATCTGAC
TTTGAGAGGGTGAGCGAGCTTGACACAAGGGATGGAAAACCTCAAGGTGTTTCCCTTCAGAACGGACATGG
GGCTCGTGTACTCCGCCTCGGAGGTTGCCGTCTGCAGGGCTGGAGCCGGGACTATATCCGAGCTCTCCTAC
TTTGAAGTACCAGCCGTCCTCATACCTTACCCTACGCCTCCGGAGACCACCAGTTTTTACAACGCCAGAGAG
ATTGAGGAGCTTGAGGCGCCTTCACGCTCAGAGCGGCGGCGGTAACCTTGATAGGGTGGTAGCCCTCG
TTGACAGGGTCTTCGCAAACATAGCGTCCATGAAGGCGAGCATAAAGAGCTTCGCCAACCCGACGGCGTC
GGAGCTAATCCTCAACGAGGTTCTTGAGGACTGAGAATTCGAAT

A.2 His6-*Hy*MurG SM2 Protein Sequence

ATGCACCACCACCACCACCACGGTCTGGTCCGCGTGGTCTAGGCTTCTCGTATCAGGAGGAGGAACAGG
AGGACACTTCTTCCCAGCTCTTGAGGTTCTCGCGAGAGCCGCGGCGGGCAGGCGGGCATACTACCCTCTACGTAG
GCGCCCAGAGAGGCATAGAGAGGGGCTTTGAGCACGCCATACCCGGTGCGGCGCTCTTCTTGAGCTTTA
CCCCTTCAGGGGGGTATCCGTTGGAGCACGGGTGGCGGCCCTACTGAGCTTCTGGAGAGGTATTTCCATT
TGAGGAGCCATACGCAGGGGGATTTAGGACGCTCGTATTCGGAGGTTATCCGAGTGTTCCAGCCGGTGT
TCACACGGTCCTCAAGAGAAAGCCCCTTACCTGCACGAACAGAACTCAGTGCCGAGCATGACCAACAGAC
TCCTCTCCCATTTCCGAGGAAGGTCTTTATAACCTTTGAGCACTCACGGAAGTCTTCAGGGGCATGAAG
GTGGTAAGGACAGGACTGCCGATAAGGGAAGAGCTCATAAACACCGCGCTTGACAAGTCCAACGCCAAG
GAAGCGCTCGGCTTCAAACCTGAGGCACCCCTGGTGCTTTCATGGGCGGCAGTCAGGGGGCAAGATTTA
TAAACAACCTCGCGGTAGACTTCGCCAAGAAGACCGGCGCACCGGTTCTGCTCTTGCTGGAGAATCTGAC

TTTGAGAGGGTGAGCGAGCTTGCACAAGGGATGGAAAACCTCAAGGTGTTCCCTTCAGAACGGACATGG
 GGCTCGTGTACTCCGCCTCGGAGGTTGCCGTCTGCAGGGCTGGAGCCGGGACTATATCCGAGCTCTCTAC
 TTTGAAGTACCAGCCGTCCTCATACTTACCCCTACGCCTCCGGAGACCACCAGTTTTACAACGCCAGAGAG
 ATTGAGGAGCTTGGAGGCGCCTTCACGCTCAGAGCGGCGGCGGTAAACCTTGATAGGGTGGTAGCCCTCG
 TTGACAGGGTCTTCGCAGCAGCAGCATCCATGAAGGCGAGCATAAAGAGCTTCGCCAACCCGACGGCGTC
 GGAGCTAATCCTCAACGAGGTTCTTGAGGACTGAGAATTCGAAT

A.3 His6-*Hy*MurG Mutant 17 Protein Sequence

ATGCACCACCACCACCACCACGGTCTGGTCCGCGTGGTCTAGGCTTCTCGTATCAGGAGGAGGAACAGG
 AGGACACTTCTCCAGCTCTTGAGGTTCTCGCGAGAGCCGCGGCGGGCAGGATACCTACCCTCTACGTAG
 GCGCCCAGAGAGGCATAGAGAGGGGCTTTGAGCACGCCATACCCGGTGCGGCGCTCTTCTTGAGCTTTA
 CCCCTTCAGGGGGTATCCGTGCAAGCACGGTGGCGGCCCTACTGAGCTTCTGGAGAGGTATTTCCATT
 TGAGGAGCCATACGCAGGGGATTTGAGGACGCTCGTATTCGGAGGTTATCCGAGTGTTCCAGCCGGTGT
 TCACACGGTCTCAAGAGAAAGCCCCTCTACCTGCACGAACAGAACTCAGTGCCGAGCATGACCAACAGAC
 TCCTCTCCATTTCCGAGGAAGGTTTATAACCTTTGAGCACTCACGGAAGTTCTTCAGGGGCATGAAG
 GTGGTAAGGACAGGACTGCCGATAAGGGAAGAGCTATAAACACCGCGCTTGACAAGTCCAACGCCAAG
 GAAGCGCTCGGCTTCAAACCTGAGGCACCCCTGGTGTCTTCATGGCGGCAGTCAGGGGGCAAGATTTA
 TAAACAACCTCGCGGTAGACTTCGCCAAGAAGACCGGCGCACCGGTTCTGCTCTTGCTGGAGAATCTGAC
 TTTGAGAGGGTGAGCGAGCTTGCACAAGGGATGGAAAACCTCAAGGTGTTCCCTTCAGAACGGACATGG
 GGCTCGTGTACTCCGCCTCGGAGGTTGCCGTCTGCAGGGCTGGAGCCGGGACTATATCCGAGCTCTCTAC
 TTTGAAGTACCAGCCGTCCTCATACTTACCCCTACGCCTCCGGAGACCACCAGTTTTACAACGCCAGAGAG
 ATTGAGGAGCTTGGAGGCGCCTTCACGCTCAGAGCGGCGGCGGTAAACCTTGATAGGGTGGTAGCCCTCG
 TTGACAGGGTCTTCGCAAACATAGCGTCCATGAAGGCGAGCATAAAGAGCTTCGCCAACCCGACGGCGTC
 GGAGCTAATCCTCAACGAGGTTCTTGAGGACTGAGAATTCGAAT

A.4 His6-*Alg14*TMD-*Hy*MurG Protein Sequence

ATGCACCACCACCACCACCACGGTCTGGTCCGCGTGGTCTAGGCTTCTCGTATCAGGAGGAGGAACAGG
 AGGACACTTCTCCAGCTCTTGAGGTTCTCGCGAGAGCCGCGGCGGGCAGGATACCTACCCTCTACGTAG
 GCGCCCAGAGAGGCATAGAGAGGGGCTTTGAGCACGCCATACCCGGTGCGGCGCTCTTCTTGAGCTTTA
 CCCCTTCAGGGGGTATCCGTTGGAGCACGGTGGCGGCCCTACTGAGCTTCTGGAGAGGTATTTCCATT

TGAGGAGCCATACGCAGGGGGATTTTCAGGACGCTCGTATTCGGAGGTTATCCGAGTGTTCCAGCCGGTGT
 TCACACGGTCCTCAAGAGAAAGCCCTCTACCTGCACGAACAGAAGTCTAGTGCCGAGCATGACCAACAGAC
 TCCTCTCCCATTTTCGGCAGGAAGGTCTTTATAACCTTTGAGCACTCACGGAAGTTCTTCAGGGGCATGAAG
 GTGGTAAGGACAGGACTGCCGATAAGGGAAGAGCTCATAAACACCCGCGCTTGACAAGTCCAACGCCAAG
 GAAGCGCTCGGCTTCAAACCTGAGGCACCCCTGGTGTCTTCATGGGCGGCAGTCAGGGGGCAAGATTTA
 TAAACAACCTCGCGGTAGACTTCGCCAAGAAGACCGGCGCACCCGGTCTGCTCTTGCTGGAGAATCTGAC
 TTTGAGAGGGTGAGCGAGCTTGCACAAGGGATGGAAAACCTCAAGGTGTTTCCCTTCAGAACGGACATGG
 GGCTCGTGTACTCCGCCTCGGAGGTTGCCGTCTGCAGGGCTGGAGCCGGGACTATATCCGAGCTCTCCTAC
 TTTGAAGTACCAGCCGTCCTCATACCTTACCCCTACGCCTCCGGAGACCACAGTTTTTACAACGCCAGAGAG
 ATTGAGGAGCTTGGAGGCGCCTTCACGCTCAGAGCGGCGGCGGTAAACCTTGATAGGGTGGTAGCCCTCG
 TTGACAGGGTCTTCGCAAACATAGCGTCCATGAAGGCGAGCATAAAGAGCTTCGCCAACCCGACGGCGTC
 GGAGCTAATCCTCAACGAGGTTCTTGAGGACTGAGAATTCGAATCGCCTCGGGAAAGCCTGAGGCTTCTC
 GTATCAGGAGGAGG

A.5 His6-*EcMurG* Protein Sequence

ATGGGCAGCAGCCATCACCATCATCACACAGCCAGGATCCGAGTGGTCAAGGAAAGCGATTAATGGTGA
 TGGCAGGCGGAACCGGTGGACATGTATTCCCGGGACTGGCGGTTGCGCACCATCTAATGGCTCAGGGTTG
 GCAAGTTCGCTGGCTGGGGACTGCCGACCGTATGGAAGCGGACTTAGTGCCAAAACATGGCATCGAAATT
 GATTTCAATTCGTATCTCTGGTCTGCGTGGAAGGTATAAAGCACTGATAGCTGCCCCGCTGCGTATCTTC
 AACGCCTGGCGTCAGGCGCGGGCGATTATGAAAGCGTACAAACCTGACGTGGTGTCTCGGTATGGGAGGC
 TACGTGTCAGGTCCAGGTGGTCTGGCCGCGTGGTCTGTTAGGCATTCCGGTGTACTTCATGAACAAAACGG
 TATTGCGGGCTTAACCAATAAATGGCTGGCGAAGATTGCCACCAAAGTGATGCAGGCGTTTCCAGGTGCTT
 TCCCTAATGCGGAAGTAGTGGGTAACCCGGTGCCTACCGATGTGTTGGCGCTGCCGTTGCCGAGCAACG
 TTTGGCTGGACGTGAAGGTCCGGTTCGTGTGCTGGTAGTGGGTGGTTCTCAGGGCGCACGCATTCTTAACC
 AGACAATGCCGAGGTTGCTGCGAAACTGGGTGATTCAGTCACTATCTGGCATCAGAGCGGCAAAGTTTC
 GCAACAATCCGTTGAACAGGCGTATGCCGAAGCGGGGCAACCCGAGCATAAAGTGACGGAATTTATTGAT
 GATATGGCGGCGGCGTATGCGTGGGCGGATGTCGTGTTTTGCCGCTCCGGTGCCTAACGGTGAGTGAAA
 TCGCCGCGGCAGGACTACCGGCGTTGTTTGTGCCGTTTCAACATAAAGACCGCCAGCAATACTGGAATGCG
 CTACCGCTGGAAAAAGCGGGCGCAGCCAAAATTATCGAGCAGCCACAGCTTAGCGTGGATGCTGTGCCA

ACACCCTGGCCGGGTGGTCGCGAGAAACCTTATTAACCATGGCAGAACGCGCCCGCTGCATCCATTCCG
GATGCCACCGAGCGAGTGGCAAATGAAGTGAGCCGGGTTGCCCGGGCGTAA

A.6 His6-*HyMraY* Protein Sequence

ATGCATCACCATCACCATCACATGATATACCATCTTGCCATACTCCTGAGGGAGCACTTCTTCGCCTTCAACG
TGCTCAAGTACATAACCTTCCGTTCTTTCACGGCAATACTCCTCGCCTTCTTTATAACTCTGATACTTTCCCC
ACCTTCATGAAGAAGTTTGCGAAGATACAGAGACTTTCGGAGGGTACGTCAGAGAGTACACACCCGAAC
ACCACGAGAGCAAGAAGTACACACCAACCATGGGCGGGGTTGTGATAGTAACGGTCATACTGATAACCTC
AGTCCTTCTCATGCGCCTTGATATCAGGTACACGTGGGTTCTCGTCTTTTCAACGCTGTCCTTTGCCCTCATA
GGGTTTCGTGGACGACTGGATAAACTCAAGAATAAAAAGGGTCTCTCAATAAAGGCGAAGCTCGCCTTCC
AGATGTCCTTCGCTTAGCCGTATCCCTGCTCATCTTTACTGGGTTGGTCTGGAGACAAAGCTATACTTTCC
CTTCTCAAGGAGCTCACCGTAGATCTGGGCTGGTTATATATACCCTTCTCAATGTTTCATCATAGTAGGGAC
CGCTAACGCGGTGAACCTTACCGACGGTCTGGACGGACTCGCCATAGGTCCTTCAATGACCACAGCAACAG
CCTTCGGCGTGATAGCCTACGTGGTGGTCACTCAAAGATAGCCAGTACTTGGGAGTCCCGCACGTTCCC
TACGCAGGTGAGATAACGGTGTCTGCTTCGCGATAATAGGTGCAGGGCTTGGCTTTTTGTGGTTCAACAC
TTACCCGGCTCAGGTGTTTCATGGGAGACGTGGGAGCTCTGGGTCTCGGGGCTGCCCTCGCCACGGTTTCA
ATTATGACCAAGTCAGAGTTCCTGCTCGCCGTTGCCGGAGGTGTGTTTCGTATTTGAGACGGTAACCGTGAT
ACTTCAGATAATCTACTTCAGAGCCACAGGAGGGAAGAGGCTCTTCAGAAAGGCTCCCTTCCACCACCACC
TTGAGGAGAAGGGGCTGGACGAACCAAGATAGTGGTGAGGATGTGGATAGTTTCAGCCCTGCTCGCCAT
AGTGTCAGTGCGATGCTGAAGCTCAGG TAA

A.7 *HyMraY*-GFP Protein Sequence

ATGATATACCATCTTGCCATACTCCTGAGGGAGCACTTCTTCGCCTTCAACGTGCTCAAGTACATAACCTTCC
GTTCTTTCACGGCAATACTCCTCGCCTTCTTTATAACTCTGATACTTTCCCCACCTTCATGAAGAAGTTTGCG
AAGATACAGAGACTTTCGGAGGGTACGTCAGAGAGTACACACCCGAACACCACGAGAGCAAGAAGTAC
ACACCAACCATGGGCGGGGTTGTGATAGTAACGGTCATACTGATAACCTCAGTCCTTCTCATGCGCCTTGA
TATCAGGTACACGTGGGTTCTCGTCTTTTCAACGCTGTCCTTTGCCCTCATAGGGTTCGTGGACGACTGGAT
AAAACCTCAAGAATAAAAAGGGTCTCTCAATAAAGGCGAAGCTCGCCTTCCAGATGTCCTTCGCTTTAGCCG
TATCCCTGCTCATCTTTACTGGGTTGGTCTGGAGACAAAGCTATACTTTCCCTTCTTCAAGGAGCTCACCGT
AGATCTGGGCTGGTTATATATACCCTTCTCAATGTTTCATCATAGTAGGGACCGCTAACGCGGTGAACCTTAC

CGACGGTCTGGACGGA CTGCCATAGGTCCTTCAATGACCACAGCAACAGCCTTCGGCGTGATAGCCTACG
 TGGTGGGCTCACTCAAAGATAGCCCAGTACTTGGGAGTCCCGCACGTTCCCTACGCAGGTGAGATAACGGT
 GTTCTGCTTCGCGATAATAGGTGCAGGGCTTGGCTTTTTGTGGTTCAACACTTACCCGGCTCAGGTGTTTAT
 GGGAGACGTGGGAGCTCTGGGTCTCGGGGCTGCCCTGCCACGTTTTCAATTATGACCAAGTCAGAGTTC
 CTGCTCGCCGTTGCCGGAGGTGTGTTTCGTATTTGAGACGGTAACCGTGATACTTCAGATAATCTACTTCAGA
 GCCACAGGAGGGAAGAGGCTCTTCAGAAAGGCTCCCTTCCACCACCACCTTGAGGAGAAGGGGCTGGAC
 GAACCCAAGATAGTGGTGAGGATGTGGATAGTTTCAGCCCTGCTCGCCATAGTGTCAGTGGCGATGCTGA
 AGCTCAGG

A.8 *Ec*MraY-His6 Protein Sequence

ATGTTAGTTTGGCTGGCCGAACATTTGGTCAAATATTATTCCGGCTTTAACGTCTTTTCTATCTGA
 CGTTTCGCGCCATCGTCAGCCTGCTGACCGCGCTGTTTCATTGTGGATGGGCCCGCGTATG
 ATTGCTCATTGCAAAACTTTCTTTGGTCAGGTGGTGCCTAACGACGGTCCTGAATCACACTTC
 AGCAAGCGCGGTACGCCGACCATGGGCGGGATTATGATCCTGACGGCGATTGTGATCTCCGTAC
 TGCTGTGGGCTTACCCGTCCAATCCGTACGTCTGGTGCCTGTTGGTGGTGGTGGTAGGTTACGGT
 GTTATTGGCTTTGTTGATGATTATCGCAAAGTGGTGCCTAAAGACACCAAAGGGTTGATCGCTCG
 TTGGAAGTATTTCTGGATGTCGGTCATTGCGCTGGGTGTCGCCTTCGCCCTGTACCTTGCCGGCAA
 AGACACGCCCCGAACGCAGCTGGTGGTCCCATTCTTTAAAGATGTGATGCCGCAGCTGGGGCTG
 TTCTACATTCTGCTGGCTTACTTCGTTCATTGTGGTACTGGCAACGCGGTAAACCTGACCGATGGT
 CTCGACGGCCTGGCAATTATGCCGACCGTATTTGTCGCCGGTGGTTTTGCGCTGGTGGCGTGGGC
 GACCGGCAATATGAACTTTGCCAGCTACTTGCATATACCGTATCTGCGACACGCCGGGAACTGG
 TTATTGTCTGTACCGGATAGTCGGGGCAGGACTGGGCTTCTGTGGTTTAAACACCTATCCGGCG
 CAGGTCTTTATGGGCGATGTAGGTTGCTGGCGTTAGGTGGTGCCTTAGGCATTATCGCCGTA
 GCTACGTCAGGAATTCCTGCTGGTATTATGGGGGGCGTGTTTCGTGGTAGAAACGCTTTCTGTCA
 TCCTGCAGGTCGGCTCCTTTAAACTGCGCGGACAACGTATTTTCCGCATGGCACCGATTATCACC
 ACTATGAACTGAAAGGCTGGCCGGAACCGCGCGTCATTGTGCGTTTCTGGATTATTTGCTGATG
 CTGGTTCTGATTGGTCTGGCAACGCTGAAGGTACGTCTCGAGCACCACCACCACCACCTGA